Future benefits of high-density radiance data from MTG-IRS in the AROME fine-scale forecast model Final Report

Stephanie Guedj, Vincent Guidard, Benjamin Ménétrier, Jean-Francois Mahfouf, Florence Rabier

Future benefits of high-density radiance data from MTG-IRS in the AROME fine-scale forecast model

Final Report

Stephanie Guedj*, Vincent Guidard,
Benjamin Ménétrier, Jean-Francois Mahfouf
and Florence Rabier

CNRM-GAME/METEO-FRANCE and CNRS
42 av. Gaspard Coriolis, 31057 Toulouse, FRANCE
*: stephanie.guedj@meteo.fr

November 24, 2014

Contents

Aknowledgements

This research is funded by EUMETSAT. The authors would like to thank Pascal Brunel from the CMS for RTTOV and the IRS coefficient file. Jean Maziejewski for his help to revise the manuscript.

Abstract

1 Introduction

The accuracy of Numerical Weather Prediction (NWP) models depends largely on the availability and quality of meteorological observations. Conventional data from networks of weather stations, radio-sounding data as well as radar reflectivity and aircraft measurements provide the largest amount for convective-scale data assimilation systems. But, this observing system is supplemented by an increasingly important set of satellite observations. The next generation of EUMETSAT geostationary meteorological satellites, Meteosat Third Generation (MTG), will bring in orbit for the first time, an hyperspectral Infrared (IR) instrument, called Infrared Sounder (IRS). This instrument will provide unprecedented high-resolution geophysical information over Europe [Tjemkes et al., 2007]. Radiances will be measured inside the water vapour and CO_2 absorption bands with extremely high spectral resolution ($0.625cm^{-1}$) and accuracy ($\sim$ 2 km resolution with 10% accuracy for humidity and $\sim$ 1 km with 0.5^o-1.5^oK accuracy for temperature). The IRS spectrometer will be based on an imaging Fourier-transform interferometer, measuring radiances in two bands, 800 spectral channels in the Long-Wave InfraRed (LWIR) and 920 channels in the Mid-Wave InfraRed (MWIR), with a spatial resolution of 4 km and a basic repeat cycle of 60 min.

The purpose of this study is to evaluate the potential benefits of high-density radiance data assimilation from MTG-IRS in a fine-scale forecast model. The standard way to undertake such a study is to carry out an Observing System Simulation Experiment (OSSE) using a known artificial "truth" referred to the Nature Run (NR). It is usually defined by a global free-run model integration or a reanalysis (figure 1,[Masutani et al., 2010]). The French global Action de Recherche Petite Echelle Grande Echelle (ARPEGE) system is used to construct the NR in an especially designed high resolution configuration (7 km, 115 vertical levels). The full dataset of available observations over Europe is simulated from the NR as well as the new IRS observing system. Because observations extracted from the NR, are "perfect", various sources of error must be simulated and added to form synthetic observations [Errico et al., 2013]. Then, synthetic observations are assimilated in the same way as real observations in the 3D-Var Applications of Research to Operations at MEsoscale (AROME) system ([Seity et al., 2010] and [Brousseau et al., 2008]). This system has been operational since 2008. It is used to avoid the fraternal twin ("incest") problems, as shown in [Arnold Jr and Dey, 1986]. Indeed, both models do not use the same physic package : Schemes for deep convection, micro-physical species, shallow convection, radiative transfer and turbulence are different as well as the surface treatments). Even if some even if part of the code is common, the forecast model used for the NR is not used afterwards for the data assimilation experiment in the full OSSE. That way, the OSSE results should not show an unrealistic observation impact when compared to the "truth" when producing analyse and forecast fields.

The second purpose of this work is to tackle problems related to the general underused of satellite radiances in data assimilation systems. It is expected that NWP centres should be ready to treat the very large amount of observations produced by

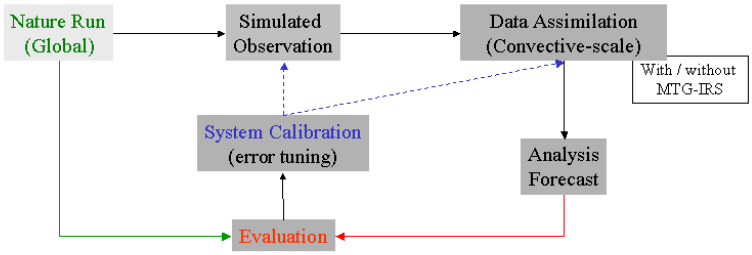

Figure 1: Observing System Simulation Experiment (OSSE) methodology

MTG-IRS to wit, ($\sim$ 3 Gigabytes/second at instrument output, [Donny and Aminou, 2014]). In addition to operational time constraints and computational processing power limitations, variational assimilation schemes also require a drastic reduction of data density. In fact, it was shown that assimilating high-density observation may result in a degradation of the analysis rather than in an improvement if the system is sub-optimal, i.e. observation/background errors are not well specified ([Liu and Rabier, 2002] and [Dando et al., 2007]). Firstly, most of NWP centres still use a diagonal observation covariance error matrix ($\mathbf{R}$), which assumes uncorrelated observational errors. This assumption is no longer valid for satellite observations which may be spectrally or spatialy correlated ([Stewart et al., 2008], [Bormann et al., 2010], [Guedj et al., 2013] among many others). Secondly, sub-optimality may arise from the use of a static, homogeneous and isotropic background covariance error matrix ($\mathbf{B}$). Background-error covariances have a deep impact on the analysis, since they are used to filter and propagate information provided by observations [Daley, 1991]. Recently, the use of correlated observation errors, as diagnosed by the Desroziers diagnostic [Desroziers et al., 2009] for Infrared Atmospheric Sounding Interferometer (IASI) was tested in assimilation trials at ECMWF and the MetOffice. The treatment of the correlated errors for IASI in 4D-Var leads to an improvement in forecast accuracy [Weston et al., 2014], providing that diagnosed variance errors are sufficiently inflated [Bormann et al., 2014]. This mean that sources of observational error correlation are not fully understood yet.

At Météo-France, OSSEs were implemented using both operational NWP models: ARPEGE for the NR and AROME for the data assimilation scheme (section 2). The full dataset of atmospheric observations, as well as MTG-IRS radiances were simulated from the NR with scaled observation errors (section 3). The section 4 presents validation and calibration exercises against real world data assimilation systems to ensure a realistic impact of the new observing system. Finally, several assimilation trials were undertaken to evaluate the the potential benefits of different-density radiance data from MTG-IRS (section 5). Potential effect of error correlations on NWP performances are discussed in section 6.

2 The Nature Run and the assimilation system used for the OSSE

2.1 The global ARPEGE forecast system

The ARPEGE system is used in operations at Météo-France for NWP since 1992. The code is partly common with the Integrated Forecasting System (IFS) software and it is used to create the NR which is a long, uninterrupted forecast representing the "true" state of the atmosphere. ARPEGE is a global spectral model, with a Gaussian grid for the grid-point calculations. The vertical discretisation is done according a following-terrain pressure hybrid coordinate over 115 vertical levels (from 0.1hPa to 10m). The version used to generate the ARPEGE-NR has a variable horizontal resolution with truncation Tl1198 with a 2.2 stretching factor (around 7.5km over France and 36km over antipodes). This NWP model was used because 1) it is a mature NWP system with a proven forecast skill and 2) the atmospheric simulation resolves scales compatible with the future MTG-IRS observing system.

The simulated fields from the ARPEGE-NR are hourly available for both prognostic and diagnostic model fields. The period covers 2 months during winter 2013 (February to March) and 4 months during summer 2013 (June to September). The first guess is based on one atmospheric analysis produced by the operational ARPEGE-NWP system. A few weeks after the starting date, the atmospheric state of the ARPEGE-NR diverges from the one of ARPEGE NWP version. The influence of assimilated observations held in the First-Guess (FG) is progressively eradicated and the system converges toward climatologies, evolving continuously in a dynamically consistent way. Figure 2 and 3 give an example of specific humidity and temperature fields produced by the Nature Run.

The ARPEGE-NR proved its usefulness in many applications within the OSSE framework. One can extract fields of the "true" atmospheric state to evaluate the quality of the produced analysis and the forecast skills whether the new observing system is included or not. The ARPEGE-Nature Run (NR) is also a source of simulated observations.

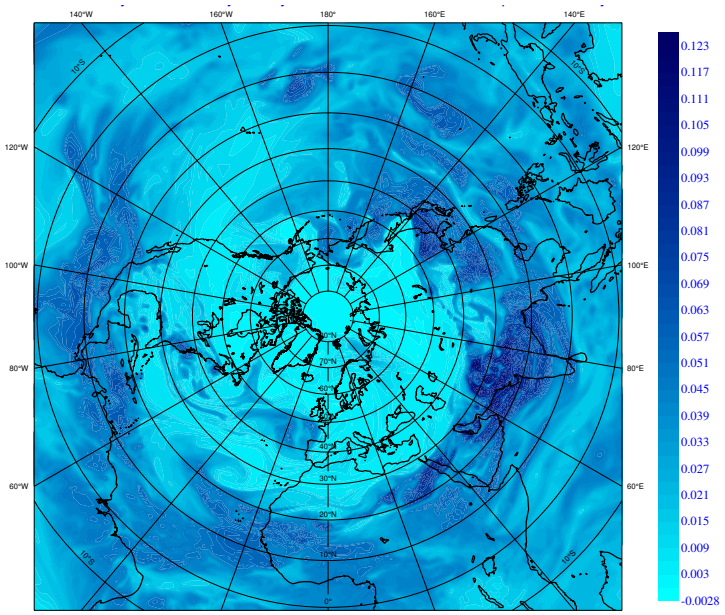

Figure 2: Maps of Specific Humidity (g/kg) from the ARPEGE Nature Run over the Northern Hemisphere, at 850 hPa,2013/07/23-00UTC, 33 days after the start run

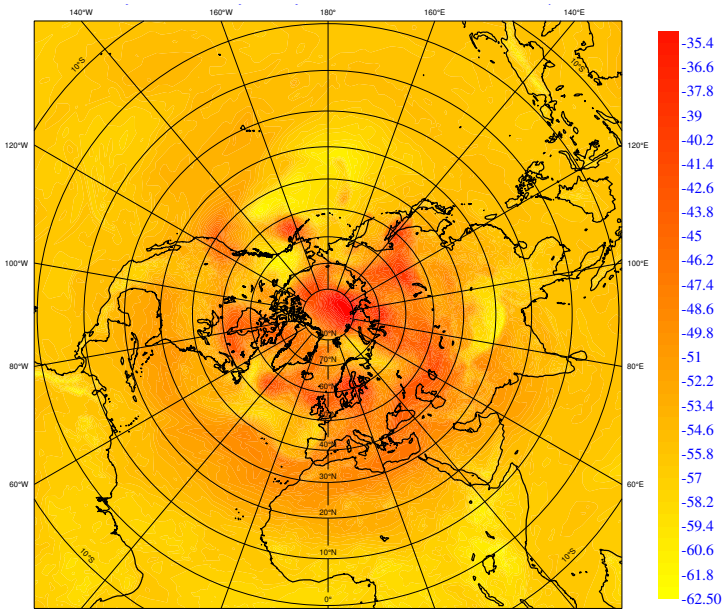

Figure 3: Maps of Temperature (^oC) from ARPEGE the Nature Run over the Northern Hemisphere, at 850 hPa,2013/07/23-00UTC, 33 days after the start run

2.2 The 3D-VAR AROME Meso-scale system

Since 2008, the AROME system is the operational convective-permitting Limited Area Model (LAM) of Météo-France with a 2.5 km-grid covering the western part of Europe and part of the Mediterranean Sea ([Seity et al., 2010]). With regard to the ARPEGE system, the AROME physical package is inherited from the physical parametrisations of the Meso-NH research model [Lafore et al., 1997]. The high horizontal resolution permits to explicitly resolve deep convection and the micro-physical scheme makes use of prognostic equations to describe the six water species. The shallow convection and turbulence are parametrised according to the Eddy Diffusivity Kain Fritsch (EDKF) scheme and the radiative scheme. Surface parameters are computed through a two-way coupling with the externalised surface model SURFEX.

The AROME system has its own data assimilation system, based on a 3D-Var scheme with an incremental formulation, observations operators, minimization technique and data flow [Courtier et al., 1998] inherited from IFS/ARPEGE and Aire Limitée Adaptation Dynamique Développement International (ALADIN) ([Fischer et al., 2005], [Brousseau et al., 2008]). The 3D-Var data assimilation system is carried out using a 3-hour forward intermittent cycle. A cycle consists in computing the analysis using observations within a $\pm$1h30 assimilation window and a 3-hour forecast to serve as FG for the next cycle. The two wind components, temperature, specific humidity and surface pressure are analysed. Other model fields are directly cycled from the previous guess. 48-h forecast can be run from each cycle.

The AROME-NWP observation error covariances are tuned to account 2 distinct contributions: instrument errors and representativeness errors. Observation errors are assumed to be uncorrelated. To compensate for this omission, 1) observation errors are inflated between 2 to 4 times that of the standard deviation of the true error covariance matrix and 2) data are dramatically thinned to insure the best observation independence. The background error covariances are based on a multivariate formulation and have been estimated using an ensemble-based method ([Berre, 2000] and [Berre et al., 2006]). In comparison with larger-scale background errors, they have smaller horizontal correlations and increased standard deviations for model parameters representing small scale structures, such as temperature in the low layers [Brousseau et al., 2008].

3 Simulation of observations

The reason for simulating observations which are to used in OSSE, is to extract observed quantities at the closest coordinate (in space and time) from the "true" background field (NR). The observation operator includes a) the interpolation process and b) the radiative transfer model RTTOV v10 ([Saunders et al., 2006]) for the direct assimilation of radiances. All observations, including MTG-IRS, are simulated (every 3 hours), from the NR, over the AROME domain.

3.1 Simulation of the operational observing systems

The averaged amount of available observation points for each assimilation cycle is :

- surface : 5000 measurements from surface stations (SYNOP), ships and buyos, 15000 observations from ground GPS (GPS-SOL) and 1000 from wind profilers.
- altitude : 950 observations from radiosondes (TEMP, PILOT, standard levels), 5000 measurements from aircraft during ascent/descent phases (AIREP, AMDAR), 3000 wind vector observations from Geostationary Orbit (GEO) and low Earth orbit (LEO) satellites, 2500 observations from LEO scatterometers (SCATT, full coverage: 9UTC, 21UTC), 1500 HIRS radiances (3UTC, 9UTC, 12UTC, 21UTC), 2000 AMSU-A and AMSU-B radiances (6UTC, 12UTC, 15UTC, 21UTC), 500 SSMI/S radiances (6UTC, 18UTC), 4000 IASI radiances, (9UTC and 21UTC), 1000 CriS radiances (3UTC, 12UTC) et 8000 Spinning Enhanced Visible and Infrared Imager (SEVIRI) radiances.

Figures 4, 5 and 6 show a comparison between simulated and real observations for conventional and radiance data. Distributions of real observations values (circles) and simulated observations over the vertical are relatively close to each other, especially for temperature. Main differences between real and simulated data occur for humidity (increase toward the surface, up to 0.77%) and U-wind profiles (increase toward the top of the atmosphere, up to 12 m/s at 200 hPa) versus real radiosounding data.

On the overall, simulated observations give satisfactory results relatively to real observations. Simulated and real observations were not expected to be exactly similar since they are not using the same atmospheric states. However, the comparison was helpful to evaluate the quality of the observation operator and the ability of the NR to describe realistically the atmosphere.

3.2 Simulation of MTG-IRS radiances

IRS will constitute spectra at a moderately high spectral resolution of 0.754 cm^{-1} with a spectral sampling of 0.625 cm^{-1} in two bands, one in the long-wave infra-red region (700 to 1210 cm^{-1}) and the other in the midwave infra-red (1600 to 2175 cm^{-1}) providing a total of 1738 channels. For operational NWP, the main focus will be on the assimilation of temperature and humidity. This work focussed on humidity channels because very

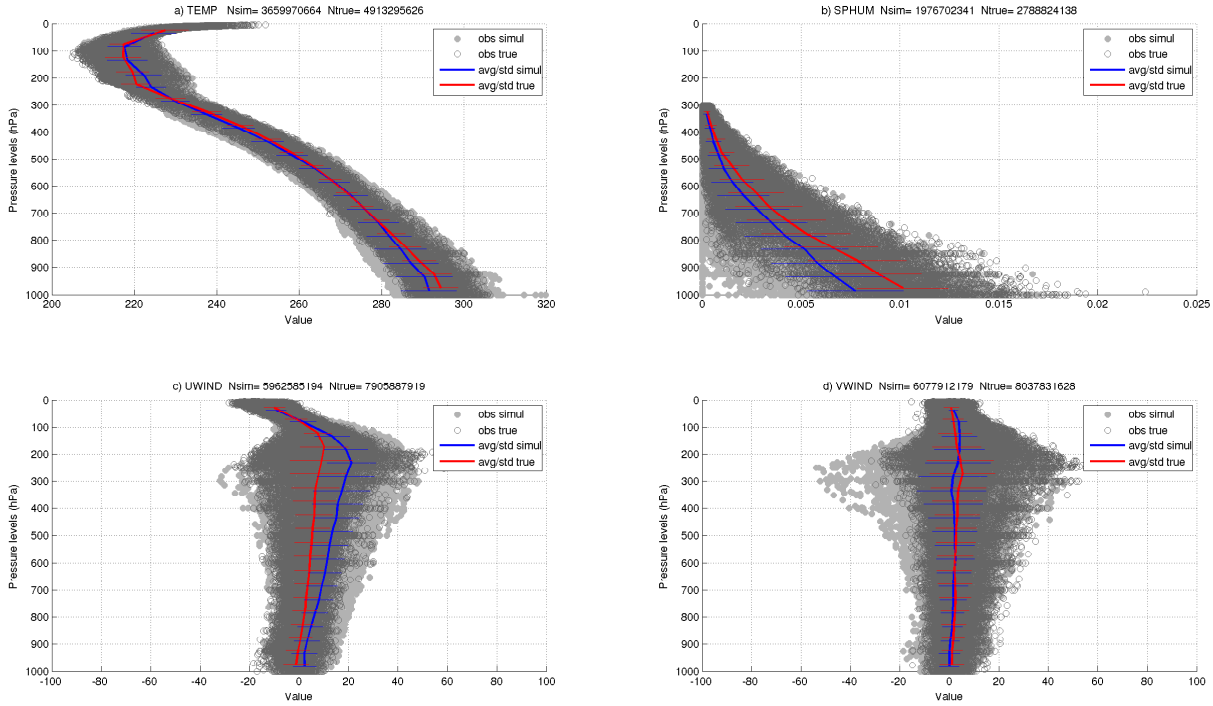

Figure 4: Simulated versus real radiosounding observation data of a) temperature , b) specific humidity and c) U and V wind components

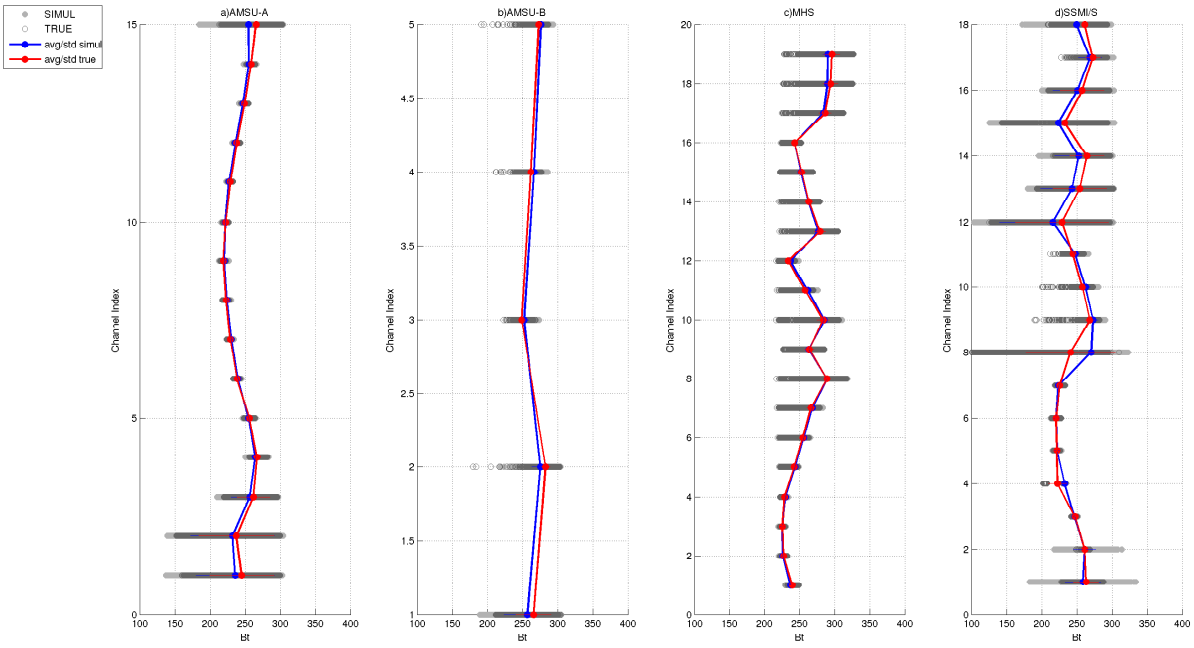

Figure 5: Simulated versus real satellite observation data of a)AMSU-A, b)AMSU-B, c) MHS, d) SSMI/S

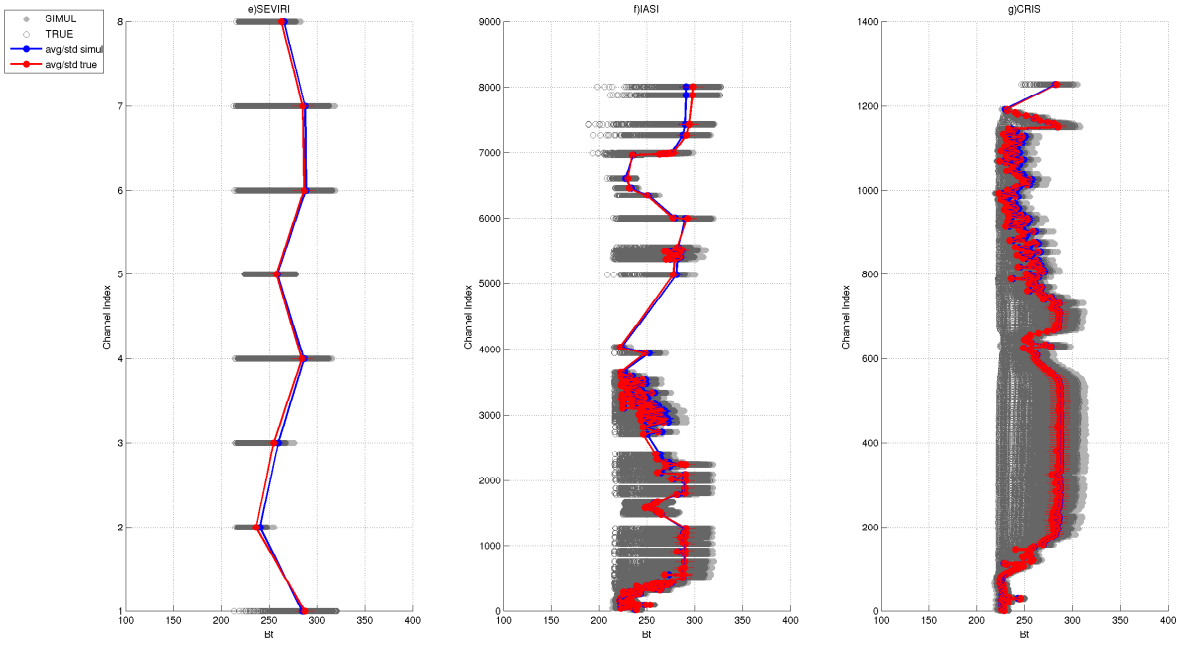

Figure 6: Simulated versus real satellite observation data of e)SEVIRI, f)IASI, g)CrIS

few channels of operational instruments (IASI CrIs ...) are efficiently assimilated.

MTG-IRS radiances were also simulated from the NR. A coefficient file for IRS was generated by Météo-France/CMS (Pascal Brunel), based on the existing IASI coefficients (more details in [Guedj et al., 2013]). In addition, most of the instrument specifications, such as observation geometry, horizontal/spatial resolution, are inherited from SEVIRI. The full IRS spectrum was simulated every 3 hours over the AROME domain.

Figure 7 shows the averaged Brightness temperature (Bt) spectrum for simulated IRS measurements. 3 channels were selected (red dots) in 1) the CO_2 absorption band (temperature sounding), 2) window band and 3) H_2O absorption band (water vapour sounding). Maps of simulated Bt for this 3 channels respectively are presented in figure 9.

It is impossible to assimilate the full spectrum, its dimensionality has to be much reduced for operational data assimilation schemes. Amidst the 640 humidity channels, we singled out 1 channel out of 5, to generate a first subset of 128 channels. Then we selected a subset of channels (50, 25 and 15) which provide information on the entire vertical (figure 9 and table 1). Then we have selected a subset of channels (50, 25 and 15) in a way that they give information on the entire vertical (figure 9, table 1). Additionally, a group of closely-separated channels circa 300 hPa were selected to evaluate in which way the system deals with redundant data. This methodology, far from optimal, strays from the original subject. This simple method was assumed to be

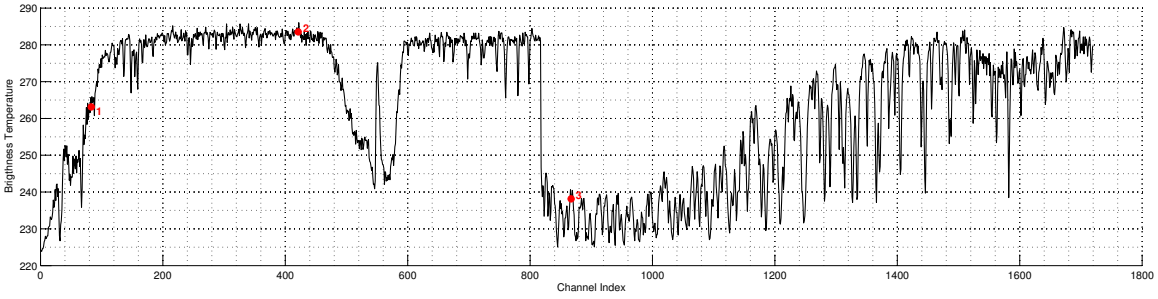

Figure 7: Averaged spectrum of simulated IRS radiances on the 25th of July 2013 - 12 UTC, over the AROME domain : 1) Temperature channel 83, 2) Window channel 421 and 3) Water Vapour channel 867

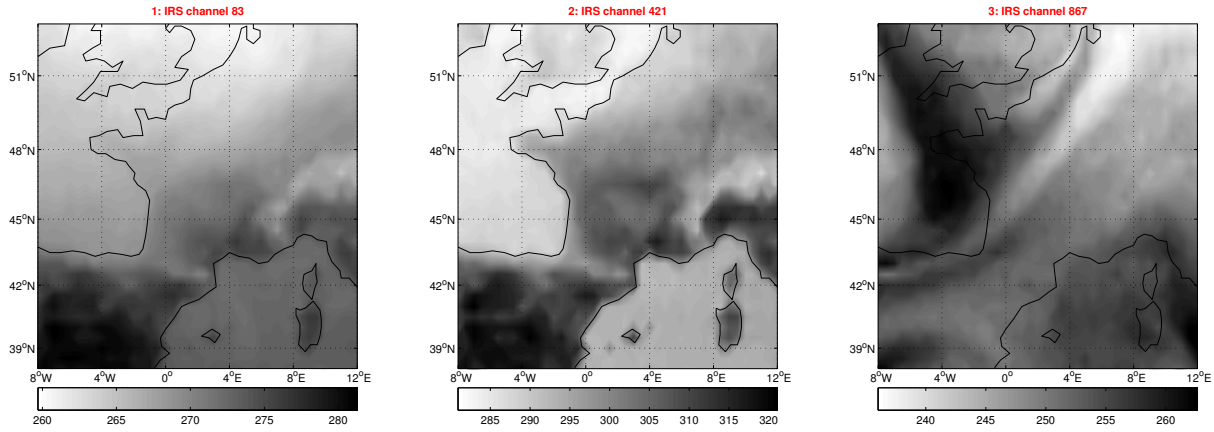

Figure 8: Maps of simulated IRS radiances on the 25th of July 2013 - 12 UTC, over the AROME domain : 1) Temperature channel 83, 2) Window channel 421 and 3) Water Vapour channel 867

sufficient at the present time .

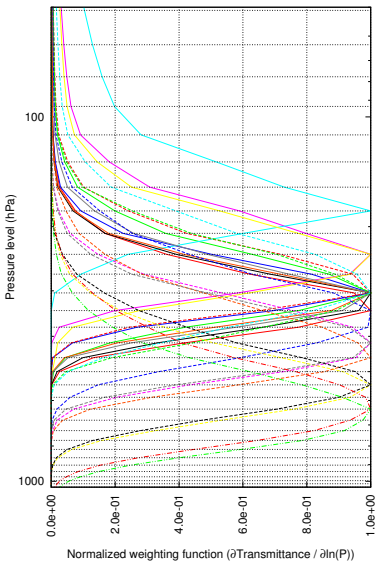

Figure 9: Normalised weighting functions for the selected 25 IRS water vapour channels

Channel Index	Central Wavenumber
915	1660.625
945	1679.375
957	1686.875
970	1695.000
978	1700.000
989	1706.875
1010	1720.000
1036	1736.250
1038	1737.500
1124	1791.250
1131	1795.625
1142	1802.500
1153	1809.375
1155	1810.625
1162	1815.000
1171	1820.625
1174	1822.500
1176	1823.750
1227	1855.625
1259	1856.875

Table 1: IRS Channel selection

3.3 Assignment of observation errors

When creating simulated observations for an OSSE, it is useful to distinguish between the modelling of observational signal and noise. The signal provides information which the data assimilation system can interpret and store, whereas any noise will be a source of error that the data assimilation system will tend to lessen.

In practice, the real observations ($\mathbf{y}$) are the sum of the true atmospheric value ($\mathbf{y}_t$) and of an error ε_m incurred during the measurement or subsequent data processing. $\mathbf{y}_t$ is also affected by an error of representativity ε_r related to the mismatch between the AROME model grid volume and the volume sampled by the instrument, as well as from a mismatch between the observed and predicted variables. In the real data assimilation system, $\mathbf{y}_t$ is unknown and ε_m is combined with ε_r. The final observation error is finally tuned up or down by the scaling factor α_1 to take into account the residual errors and correlation.

$$\underline{\text{Real Observation}} : \mathbf{y_o} = \mathbf{y}_t + ((\varepsilon_m + \varepsilon_r) \times \alpha_1)$$

In the OSSE data assimilation system, $\mathbf{y}_t$ is known (extracted from the NR) to which is added a random contribution ε_x to the model output, which stands for the observation error ($\varepsilon_x \sim \varepsilon_m + \varepsilon_r$). The random vector (actually a specific realization) is obtained from a multivariate normal distribution having the error statistics of the real observations ($\mathbf{y_o}$) and similarly scaled by the α_2 factor.

$$\underline{\text{Simulated Observation}} : \mathbf{y_s} = \mathbf{y}_t + (\varepsilon_x \times \alpha_2)$$

We can apply this methodology to the full operational observing system that needs to be assimilated in the OSSE assimilation system to construct the Control (CTL) run. But no estimate are available for MTG-IRS. Estimates from IASI and SEVIRI data were useful to specify the "correct" observation error for IRS. Three methods were used to diagnose observation errors and their correlation : the Hollingsworth and Lönnberg (H/L) method, the Desroziers (Dz) diagnostic and the Background error method. Details on methods and some results can be found in [Guedj et al., 2013]. Here we focus on both the Hollingsworth and Lönnberg (H/L) method and the Desroziers (Dz) diagnostic.

Figure 10 indicates that the observation error should be quite close to the instrument error for temperature channels. However, both methods do not show a good agreement for humidity channels. Thus, the averaged diagnosed values were interpolated following IRS expected noise function. As mentioned in [Guedj et al., 2013], IRS is expected to carry strong inter-channel/horizontal error correlation since it was diagnosed from real IASI and SEVIRI data. As our system is not sufficiently mature to take into account this error correlation/these error correlations, we have over-estimated MTG-IRS observation error on purpose, as it is done for the full operational observing system.

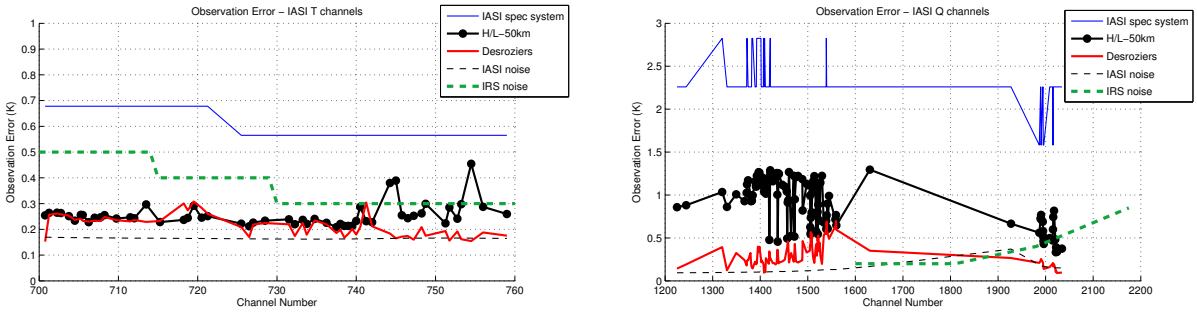

Figure 10: Estimates of observation errors (standard-deviation) for a selection of IASI T (left panel) and Q (right panel) observations : assumed observation errors (as specified in the AROME system, blue line), diagnosed values computed using the Hollingsworth and Lönnberg (H/L) method (black thick line) and using the Desroziers (Dz) diagnostic (red line). The in-flight instrument error (dashed black line) for IASI is shown as well as the recommended values for the future MTG-IRS (dotted green line).

4 OSSE calibration/validation

The statistics of analysis errors are partly determined by the statistics of observation errors, as revealed by the fundamental DAS equations and as examined further by [Daley and Ménard, 1993]. Here, the impact of simulated data in the OSSE system is verified relatively to that of real observation data in the operational system (AROME-NWP). Each observing system should ideally describe comparable impacts in the analysis and forecast skill in both systems.

Their are many methods to perform the evaluation: data denial (or adding) experiments, forecast anomaly correlation and RMS analysis/forecast error verified against the NR. In the following, results obtained from the last method are presented.
Because the assumed observation error covariances, together with background error covariances, play an important role in determining the weight of a given observation in data assimilation, several calibration/validation experiments were run to find the best possible match between the OSSE and AROME-NWP statistics (13 days, July 2013). The Operational (OPER) experiment is similar to the AROME-NWP system. Real observations were assimilated and the observation errors were not modified relatively to the operational configuration. In the CAL experiment series, observations were simulated and perturbed using scaled values of observation errors. Then, simulated observations were assimilated with the same observation errors used to simulate the observation. All assimilation experiments are summarized in table 2.

Calibration steps using analysis departures to observations/simulations of radiosonde data are presented in figure 11.

Statistics properties for the OPER run (real world) should match one of CAL experiments (OSSE world). In fact, the simulated observations should force the OSSE model state in the same way that the real observations do. The reduction of observation errors

Exp Name	Observations	Obs. error scaling factor (α)
OPER	Real	1.0
CAL-1.0	Simulated	1.0
CAL-0.8	Simulated	0.8
CAL-0.5	Simulated	0.5
CAL-0.5sc	Simulated	0.5 + manual
CAL-0.2	Simulated	0.2

Table 2: Calibration experiments

improves the fit of the OPER run down to a threshold that depends on the observation type. Figure 11 indicates that the standard deviation of observation error, as specified in the real system, should be reduced by about 50% to improve the fit between statistical properties of OSSE and the real system. Manual adjustments has been applied to low atmospheric levels.
This exercise was done for each observation type independently. Except for AMSU observations, the observational errors were/error was reduced by about 50%

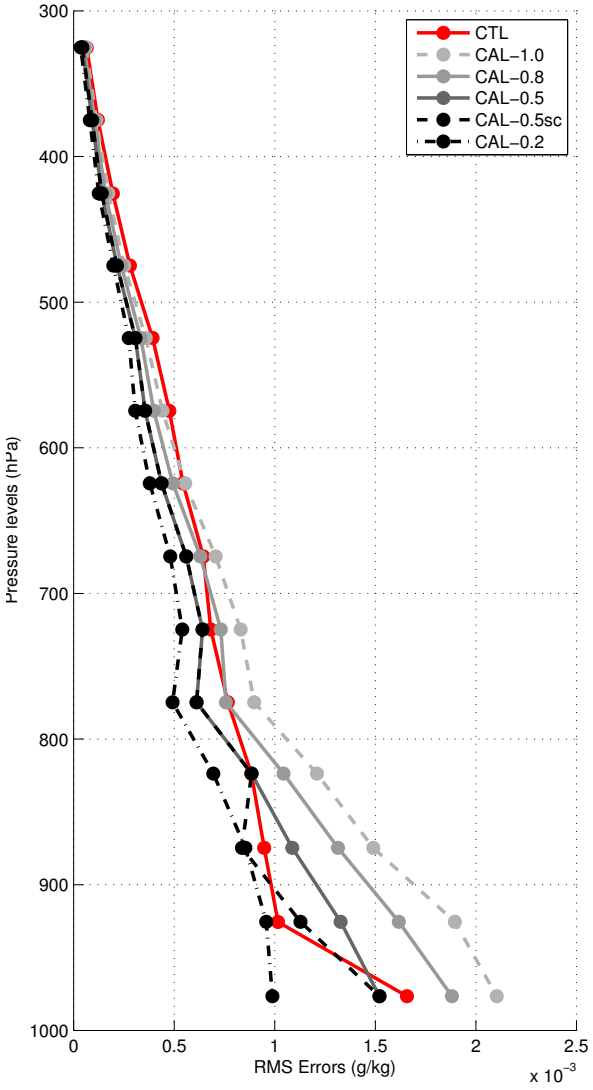

Figure 11: Analysis departures to specific humidity observations/simulations for radiosounding data following 5 configurations : 1) The CTL run assimilates real observations with the same observational error as the operational system (α_1); 2) CAL-1.0 assimilates simulated observations with the same observational error as the operational system ($\alpha_1 = \alpha_2 = 1.0$); 3) CAL-0.8 assimilates simulated observations with reduced observational error with regard to the operational system ($\alpha_2 = 0.8$); 4) CAL-0.5 assimilates simulated observations with reduced observational error with regard to the operational system ($\alpha_2 = 0.5$); 5) CAL-0.5sc assimilates simulated observations with reduced observational error with regard to the operational system and manual adaptations ($\alpha_2 = 0.5sc$); 6) CAL-0.2 assimilates simulated observations with reduced observational error with regard to the operational system and manual adaptations ($\alpha_2 = 0.2$)

5 Results : Assimilation experiments

A set of assimilation experiments was tested by the OSSE, to detect future benefits of MTG-IRS in the AROME mesoscale model.

As mentioned earlier, the full operational observing system as well as IRS radiances were simulated (section 3) with calibrated errors (section 4) during 15 days (July 2013). This set of simulated observations were assimilated with the same error used to construct the CTL run. In this experiment, simulated observations were subjected to various quality control checks such as selection of stations, levels and channels, flow-dependent background departure check, redundancy check, horizontal and vertical thinning of data denser than the model grid... Observations are also bias corrected in the operational model using the variational bias correction scheme (VarBC, [Auligné et al., 2007]). However, since synthetic observations are assumed to be unbiased in the OSSE, the VarBC scheme was disconnected: no bias correction was applied.

25 IRS humidity channels were assimilated with different thinning distances (20, 40 and 80 km), as shown in table 3. Additional experiments were also carried out using different IRS humidity channel selection (15, 25, 50 channels, not shown) or a selection of temperature channels ...

All assimilation experiments ran during 15 days (July 2013), with a 48h forecast. Since OSSEs are very labour intensive, we present here the result for the 25th of July at 12UTC with a focus on humidity impacts.

Exp Name	Distance Thinning (km)	Channel number
CTL (no IRS)		
CTL+IRS80km	80	25
CTL+IRS40km	40	25
CTL+IRS20km	20	25

Table 3: Assimilation experiments

5.1 Impacts on atmospheric analysis

In the OSSE framework, the NR can be used to verify the quality of the analysis while comparing it to the true state of the atmosphere. The full set of atmospheric specific humidity profiles (516152 profiles) were extracted every 3h, from all assimilation experiments and compared to the NR. Standard Deviation (STD), Root Mean Square (RMS) error and bias were computed over a set of analysis. Figure 12 shows analysis scores versus the NR for the CTL run (no IRS, red line), the IRS80km run (back line), IRS40km (blue line) and IRS20km (green line). The assimilation of IRS do improve specific humidity modelling from the surface to the top of the atmosphere. Mean analysis reduction errors are about 27.2% for IRS80km, 31.5% for IRS40km 27.7% for IRS20km

over whole vertical levels. The maximum impact is obtained for high atmospheric levels (800-400 hPa) where few observations are used.The IRS impact is lower outside this region because the information brought can be redundant with **SEVIRI!** (**SEVIRI!**) water vapour channels at the top and with conventional observations at the bottom.

Figure 13 shows maps of specific humidity RMS error at 700 hPa, computed against the NR. Maps of IRS observation location are also presented to illustrate used data density in each experiment. As shown in figure 13, IRS data improve the smaller spatial scales.

However, figures 12 and 13 indicate also that the system is not able to take full advantage of an increase in assimilated data density. There is a threshold where increasing assimilated data amount do not add any information to the analysis. Theoretically, this finding is relevant when real observations are assimilated at a too high density because they may carry error correlation ([Liu and Rabier, 2002] and [Dando et al., 2007], [Bormann et al., 2010]). However, in this work, errors were added to perfect observation values while ignoring correlations (section 3).

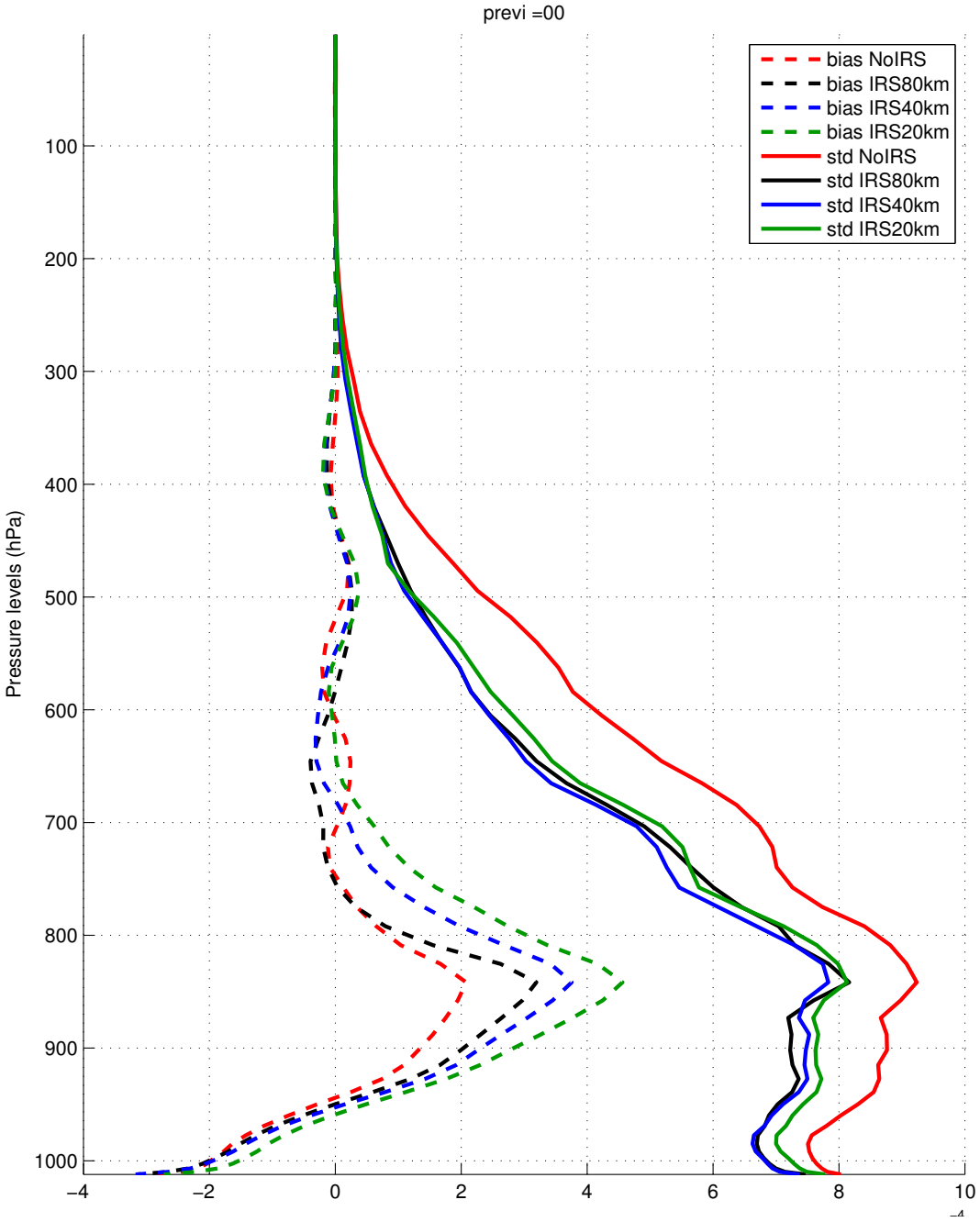

Figure 12: Analysis scores (bias and STD) of specific humidity versus the Nature Run for 4 assimilation experiments on the 25th of July - 12H

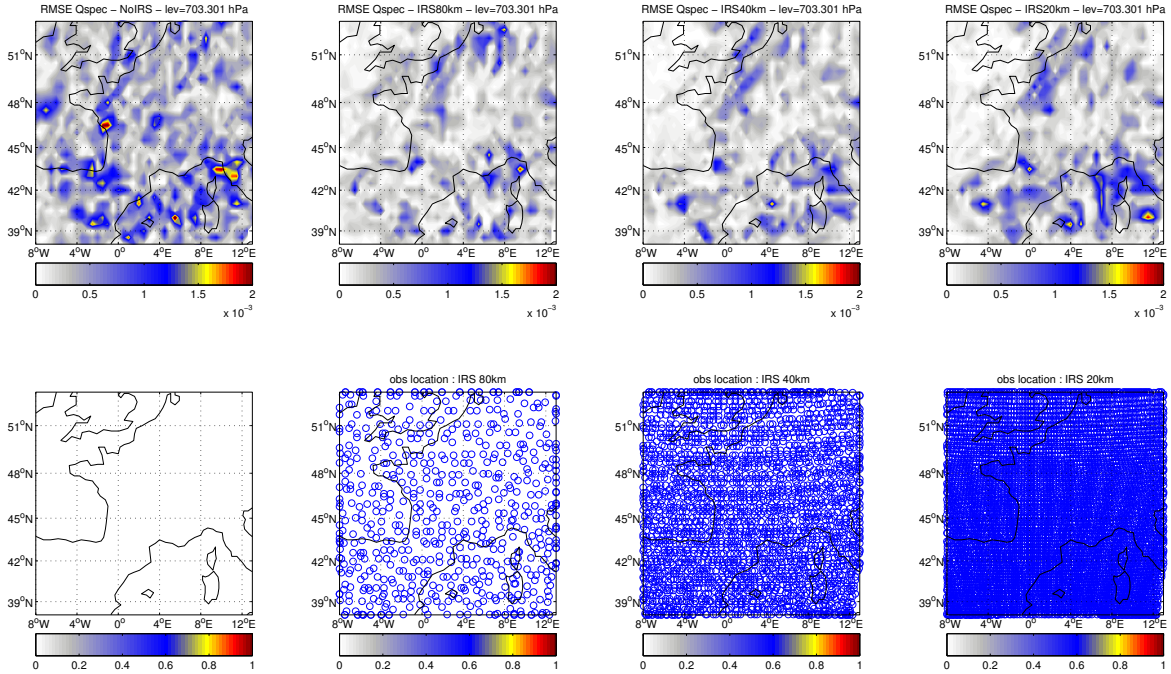

Figure 13: Analysis scores (RMS) of specific humidity (700 hPa) versus the Nature Run for 4 assimilation experiments on the 25th of July - 12H

5.2 Impacts on forecast scores

The ultimate goal of data assimilation in the meso-scale NWP context is to improve short-range forecast (3-12h), mid-range forecasts (12-24h) and longer range forecasts (24-48h). The evolution of data impact with forecasts is shown in figure 14. Time series of specific humidity forecast error (RMS) versus the NR are presented as a function of forecast ranges. Results are averaged from the surface to the top of the atmosphere for each forecast range.

Positive impacts are demonstrated on short-range forecast fields of specific humidity when IRS are assimilated. Best results are obtained using the IRS80 experiment since the improvement is visible up to 48h. However, IRS20 and IRS40 experiments show a degradation of the forecast quality from 9h and 12h respectively.

Profiles of forecast scores (STD) were computed for IRS80, IRS40 and IRS20 experiments, normalised by the CTL run (NoIRS) at 8 forecast ranges (6h, 12h, 18h, 24h, 30h, 36h,42h and 48h, figure 15). Negative (positive) values, indicate that the assimilation of IRS decrease (increase) the forecast error with regard to the NR. Error changes are expressed in %. Overall, the assimilation of IRS data induces changes in humidity profiles at all forecast ranges. IRS80 scores demonstrates neutral to positive impacts whereas IRS40 and IRS20 show negative to neutral impacts. Quantitatively, even if changes seem over-estimated, maximum changes affect short-ranges forecast (up to -33.74% of

STD error, 500 hPa) and can be sensitive up to 48h-forecast (up to +8.35% of STD error, 700 hPa).

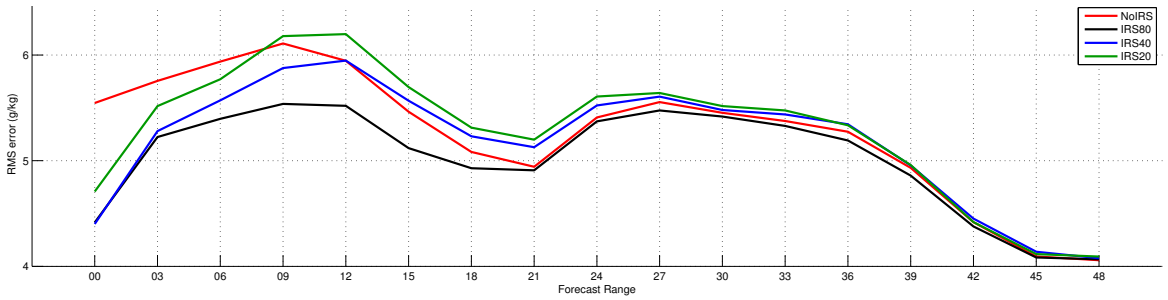

Figure 14: Forecast scores (RMSE) time series of specific humidity for 4 assimilation experiments. Forecasts are computed from the analyse fields of the 25th of July 2013. The CTL run (red line) do not assimilate IRS observations. IRS80 (blue line), IRS40 (black line) and IRS20 (green line) experiments assimilate IRS observations with a distance thinning of 80, 40 and 20 km respectively. RMS is computed against the Nature Run at corresponding time

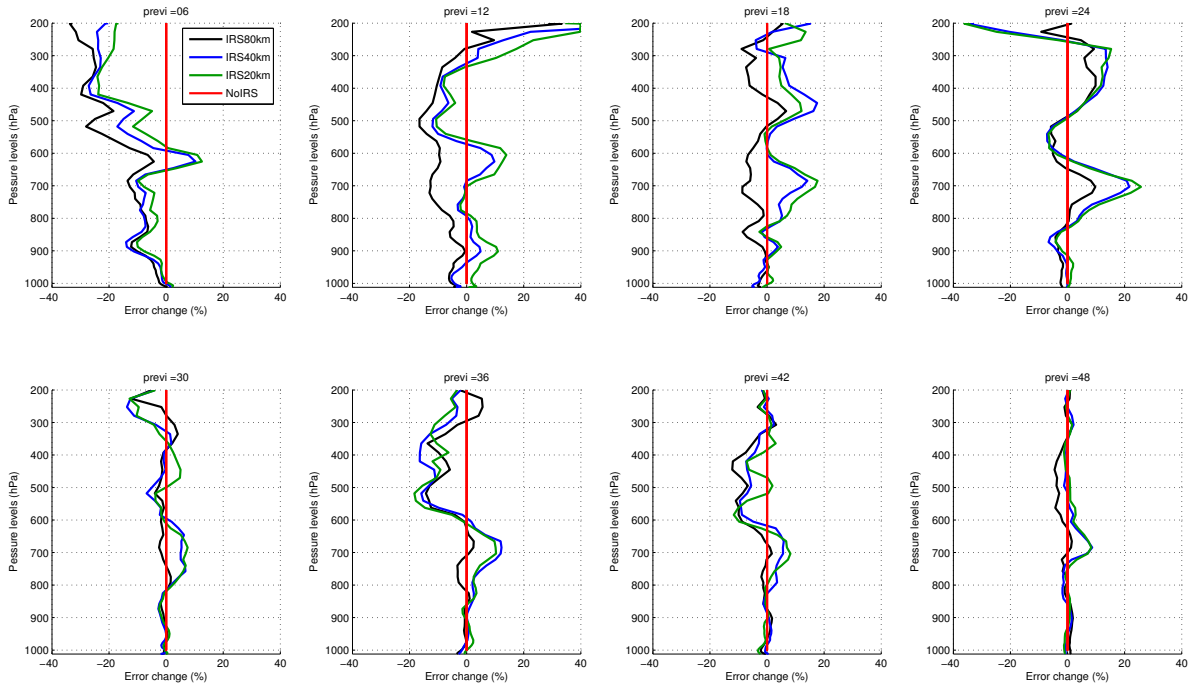

Figure 15: Normalised forecast scores (STD) profiles of specific humidity. Forecasts are computed from the analyse fields of the 25th of July 2013. The CTL run (red line) do not assimilate IRS observations. IRS80 (blue line), IRS40 (black line) and IRS20 (green line) experiments assimilate IRS observations with a distance thinning of 80, 40 and 20 km respectively. RMS is computed against the Nature Run at corresponding time and it is normalised with the CTL run. Error changes are expressed in %.

6 Discussion

To interpret OSSE results is quite challenging. The many causes of inconsistent results must be investigated carefully and explained for OSSEs to be more creditable. In our case, the assimilation system cannot extract useful information if the amount of assimilated data is too dense. The best analysis and forecast improvements of humidity fields are assigned to IRS80 whereas IRS20 get the worst results.

In this work, observations were simulated and assimilated assuming uncorrelated errors. Following studies presented in [Liu and Rabier, 2002], [Desroziers et al., 2009] and [Guedj et al., 2012], a gradual increase in data density should monotonically improve the quality of the analyses if 1) observations errors are uncorrelated and 2) the analysis is optimal. In our system, this is not verified (section 5). In order to better understand the origin of theses results, the a posteriori Desroziers diagnostic was applied on the analysis and first-guess departures to simulated observations. Unexpected and significant inter-channel error correlations were diagnosed even if they were assumed uncorrelated during the simulation/assimilation process (figure 16).

Several failures in the assimilation and diagnostic schemes can explain these unexpected results. Indeed, the Desroziers diagnostics are exact under the following conditions:

- the specified error covariance matrices (B and R) are exact,
- the analysis is optimal (true minimum of the cost function),
- the statistical expectations in Desroziers diagnostics should be computed over independent realizations.

If these conditions were met in our case where uncorrelated observation errors were explicitely specified, then the diagnosed observation error correlation matrix should be diagonal, and the first-guess departure and background error correlation matrices should be equal except for diagonal coefficients.

This is not the case here, probably because:

- the specified background error covariance matrix is a climatologic, homogeneous and isotropic model, which is a crude representation of the true background error covariance matrix,
- the analysis is determined after a limited number of iterations, so that the minimum of the cost function is not always reached,
- the statistical expectations in Desroziers' diagnostics are approximated with an homogeneous and isotropic ergodicity assumption: observation couples are sorted according to thier separation and covariances are computed inside each distance class.

Several studies have shown the limitations of Desroziers diagnostics, especially for the computation of off-diagonal coefficients. Some attempts to correct this issue with iterative schemes are currently developed. In any case, these findings should be studied further to improve our understanding in observation error correlation and its effect on NWP systems ...

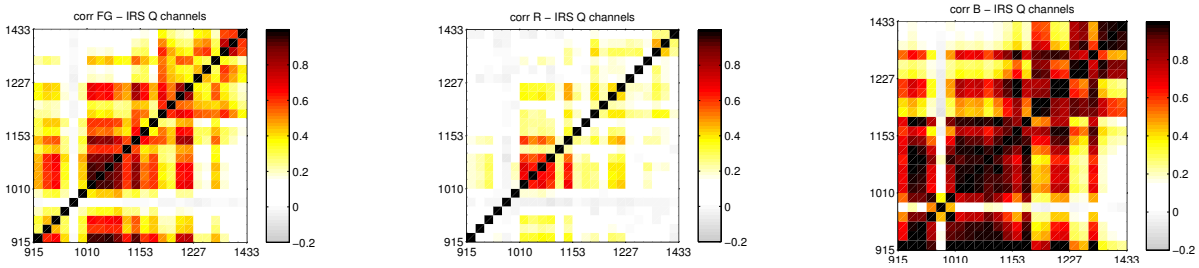

Figure 16: Error correlation matrix for a) First-guess departures to simulated IRS data, b) observations error and c) background errors (in observation space). Error correlation were diagnosed over a period of 15 days (July 2013), over the AROME domain

7 Conclusion and future plans

An Observing System Simulation Experiment (OSSE) was implemented to investigate the potential impact of the future MTG-IRS in the convective-scale AROME forecast system. In OSSE, simulated rather than real observations are the input to the 3D-Var data assimilation system. Hence, all observation types (conventional and satellite measurements) as well as IRS radiances were simulated from the true state of the atmosphere: the Nature Run (NR) (section 3). To make them more realistic, these values were explicitly increased by an appropriate amount of noise, sized on observation error (section 4). The resulting values were ingested into the data assimilation system, in the same way real observation would be in the operational system. Several configurations for the assimilation of water vapour MTG-IRS channels were evaluated as well as the CTL run in which all simulated observations are used except IRS (section 5).

An important work was undertaken for the preparation of MTG-IRS data assimilation. First, the full IRS spectrum was simulated using the RTTOV radiative transfer model. Then, an intensive inter-comparison exercise and error estimation/calibration with existing satellite measures, was conducted to ensure good quality simulations with realistic errors. Instruments such as the SEVIRI radiometer (similar time/spatial resolution) and the IASI hyper-spectral sounder (similar spectral resolution), were primarily used for these exercises. The main results show that MTG-IRS observation errors amplitude for water vapour channels, diagnosed from IASI data, should be increased by a factor of 2.5, starting from the level of radiometric noise. This result is consistent with [Bormann et al., 2014]. This factor should be even higher if one wants to take into account account the presence of inter-channel error correlation for real observations. In addition, SEVIRI were useful to evaluate the best thinning distance to use for MTG-IRS. Horizontal error correlations were diagnosed for this task and it was shown that the distance between two observations should not be higher than 40km. More details can be found in [Guedj et al., 2012] and [Guedj et al., 2013].

Then, simulated radiances of MTG-IRS were included into the system with preliminary diagnosed observation error. In practice, effective horizontal and vertical data density of IRS were modified in each experiment, playing on thinning distance and channel selection. Since this work was carried out in an OSSE framework, it was possible to evaluate the realism of produced analysed and forecast fields against the NR and the impact of MTG-IRS against the CTL run. Quantitatively, the future observing system may be able to significantly improve the specific humidity modelling, especially when few observations are available. However, forecast impact studies indicate that the density (in term of thinning distance and channel selection) should be carefully specified. The analysis improvement do not well propagated into the forecast if observations are too densely assimilated. Large Root Mean Square (RMS) error may occurs on humidity, temperature and wind fields, up to 48h forecast. Experiments simulating only the impact of observations from polar-orbiting satellites are oversimplified compared with the impacts expected from the complete global observing system. Nevertheless, they are useful as they contribute toward the forecast error reduction.

Preliminary studies on diagnosed error correlation were presented in section 6 to explain briefly potential sources of forecast changes. Recently, [Bormann et al., 2014] showed that accounting for inter-channel error correlations allows the use of an R consistent with diagnostics and slight inflation gives a small benefit. [Weston et al., 2014] shows similar results and demonstrates that accounting for inter-channel error correlations allows a more aggressive use of observations which leads to an improved forecast accuracy, as well as an adaptive weighting of the observations based on the relationship. But, does a non-diagonal R will allow the use of more water vapour channels for the future hyperspectral MTG-IRS sounders? What about the temporal error correlation ([Eyre and Weston, 2013])?

This report, as well as the litterature demonstrate current operationalNWP assimilation schemes make use of only a small fraction of the instrument potential (horizontal thinning, channel selection ...). In the same time, new generation of hyperspectral instruments are planed to deliver more and more observations : 2738 channels for MTG-IRS every hour, 16921 spectral channels for IASI-NG (New Generation). In order to reduce the spectrum into a small number of measurements, one proposed method is Principal Component (PC) compression. This method should be a greate advantage for data dissemination but, at the present time, the direct assimilation of PC scores is not recommended for operational use [Hilton and Collard, 2009]. However, the use of reconstructed radiance spectrum from PC scores is an area of active research.

References

[Arnold Jr and Dey, 1986] Arnold Jr, C. P. and Dey, C. H. (1986). Observing-systems simulation experiments: Past, present, and future. *Bulletin of the American Meteorological Society*, 67(6):687–695.

[Auligné et al., 2007] Auligné, T., McNally, T., and Dee, D. (2007). Adaptative bias correction for satellite data in a numerical weather prediction system. *Quarterly Journal of the Royal Meteorological Society*, 133:631–642.

[Berre, 2000] Berre, L. (2000). Estimation of synoptic and mesoscale forecast error covariances in a limited-area model. *Monthly weather review*, 128(3):644–667.

[Berre et al., 2006] Berre, L., Ecaterina Ştefănescu, S., and Belo Pereira, M. (2006). The representation of the analysis effect in three error simulation techniques. *Tellus A*, 58(2):196–209.

[Bormann et al., 2010] Bormann, N., Collard, A., and Bauer, P. (2010). Estimates of spatial and interchannel observation-error characteristics for current sounder radiances for numerical weather prediction. II: Application to AIRS ans IASI data. *Quarterly Journal of the Royal Meteorological Society*, 136(649):1051–1063.

[Bormann et al., 2014] Bormann, N., Collard, A., Eresmaa, R., and Bauer, P. (2014). Accounting for inter-channel observation error correlations in the ecmwf system. In *Workshop on Correlated Observation Errors in Data Assimilation, Reading, UK*.

[Brousseau et al., 2008] Brousseau, P., Bouttier, F., Hello, G., Seity, Y., Fischer, C., Berre, L., Montmerle, T., Auger, L., and Malardel, S. (2008). A prototype convective-scale data assimilation system for operation : the Arome-RUC. *HIRLAM Techn. Report*, 68:23–30.

[Courtier et al., 1998] Courtier, P., Andersson, E., Heckley, W., Vasiljevic, D., Hamrud, M., Hollingsworth, A., Rabier, F., Fisher, M., and Pailleux, J. (1998). The ecmwf implementation of three-dimensional variational assimilation (3d-var). i: Formulation. *Quarterly Journal of the Royal Meteorological Society*, 124(550):1783–1807.

[Daley, 1991] Daley, R. (1991). Atmospheric data analysis. *Cambridge University Press, Cambridge Atmospheric and Space Science Series*, 4:57.

[Daley and Ménard, 1993] Daley, R. and Ménard, R. (1993). Spectral characteristics of kalman filter systems for atmospheric data assimilation. *Monthly weather review*, 121(5):1554–1565.

[Dando et al., 2007] Dando, M., Thorpe, A., and Eyre, J. (2007). The optimal density of atmospheric sounder observations in the met office nwp system. *Quarterly Journal of the Royal Meteorological Society*, 133(629):1933–1943.

[Desroziers et al., 2009] Desroziers, G., Berre, L., and Chapnik, B. (2009). Objective validation of data assimilation systems: Diagnosing sub-optimality. In *Proceedings of the ECMWF workshop on diagnostics of data assimilation system performance. ECMWF: Reading, UK*, pages 15–25.

[Donny and Aminou, 2014] Donny, M. and Aminou, A. (2014). Meteosat third generation (mtg), space segment status and its technological challenges. In *The 2014 EUMETSAT Meteorological Satellite Conference, 22 - 26 September 2014, Geneva, Switzerland*.

[Errico et al., 2013] Errico, R. M., Yang, R., Privé, N. C., Tai, K.-S., Todling, R., Sienkiewicz, M. E., and Guo, J. (2013). Development and validation of observing-system simulation experiments at nasa's global modeling and assimilation office. *Quarterly Journal of the Royal Meteorological Society*, 139(674):1162–1178.

[Eyre and Weston, 2013] Eyre, J. and Weston, P. (2013). The impact of the temporal spacing of observations on analysis errors in an idealised data assimilation system. *Quarterly Journal of the Royal Meteorological Society*.

[Fischer et al., 2005] Fischer, C., Montmerle, T., Berre, L., Auger, L., and Ştefănescu, S. (2005). An overview of the variational assimilation in the aladin/france numerical weather-prediction system. *Quarterly Journal of the Royal Meteorological Society*, 131(613):3477–3492.

[Guedj et al., 2012] Guedj, S., Rabier, F., and Guidard, V. (2012). Future benefits of high-density radiance data from mtg-irs in the arome fine-scale forecast model, report tn-1: Satellite observation error correlations in data assimilation. Technical report.

[Guedj et al., 2013] Guedj, S., Rabier, F., and Guidard, V. (2013). Future benefits of high-density radiance data from mtg-irs in the arome fine-scale forecast model, report tn-2: Diagnostic of observation error correlations and osse implementation. Technical report.

[Hilton and Collard, 2009] Hilton, F. and Collard, A. (2009). Recommendations for the use of principal component-compressed observations from infrared hyperspectral sounders. *Met Office Forecasting R&D Technical Report*, 536.

[Lafore et al., 1997] Lafore, J., Stein, J., Asencio, N., Bougeault, P., Ducrocq, V., Duron, J., Fischer, C., Héreil, P., Mascart, P., Masson, V., et al. (1997). The meso-nh atmospheric simulation system. part i: Adiabatic formulation and control simulations. In *Annales Geophysicae*, volume 16, pages 90–109. Springer.

[Liu and Rabier, 2002] Liu, Z. and Rabier, F. (2002). The interaction between model resolution, observation resolution and observation density in data assimilation: A one-dimensional study. *Quarterly Journal of the Royal Meteorological Society*, 128(582):1367–1386.

[Masutani et al., 2010] Masutani, M., Schlatter, T. W., Errico, R. M., Stoffelen, A., Andersson, E., Lahoz, W., Woollen, J. S., Emmitt, G. D., Riishøjgaard, L.-P., and Lord, S. J. (2010). Observing system simulation experiments. In *Data Assimilation*, pages 647–679. Springer.

[Saunders et al., 2006] Saunders, R., Matricardi, M., Brunel, P., English, S., Bauer, P., OKeefe, U., Francis, P., and Rayer, P. (2006). RTTOV-8 science and validation report. Technical report, EUMETSAT/ECMWF Program Document ID NWPSAF-MO-TV-007.

[Seity et al., 2010] Seity, Y., Brousseau, P., Malardel, S., Hello, G., Bénard, P., Bouttier, F., Lac, C., and Masson, V. (2010). The arome-france convective scale operational model. 0(0):null.

[Stewart et al., 2008] Stewart, L., Dance, S., and Nichols, N. (2008). Correlated observation errors in data assimilation. *International journal for numerical methods in fluids*, 56(8):1521–1527.

[Tjemkes et al., 2007] Tjemkes, S., Grandell, J., Borde, R., and Stuhlmann, R. (2007). Capabilities of the mtg-irs candidate candidate mission to depict horizontal moisture structures. *Fourier Transform Spectroscopy/Hyperspectral Imaging and Sounding of the Environment*.

[Weston et al., 2014] Weston, P., Bell, W., and Eyre, J. (2014). Accounting for correlated error in the assimilation of high-resolution sounder data. *Quarterly Journal of the Royal Meteorological Society*.